Effect of Block Copolymer Coated Nanoclay on Polystyrene Foams under supercritical Carbon Dioxide

Weibin Zha, Bin Zhu, Jintao Yang and L. James Lee
Department of Chemical and Biomolecular Engineering
The Ohio State University

Polystrene-*b*-polymethyl methacrylate (PS-*b*-PMMA) was end-tethered on Montmorillonite (MMT) by atom transfer radical polymerization (ATRP) to make exfoliated nanoclay composites. These nanocomposites were mixed with polystyrene (PS) by melt blending. The mixtures were then batch formed with supercritical CO_2. It was found that the cell density of foams based on these blends with 1 wt% modified MMT is higher than that based on neat PS and PS compounded with neat PMMA or PS-*b*-PMMA at the same foaming conditions. The presence of nanoclay dramatically increases the viscosity of the mixture. The heterogeneous nucleation effect of the nanoclay and nanocomposites will be discussed.

Introduction

The traditional physical blowing agents for PS foams, chlorofluorocarbon (CFC), have been banned all around the world due to its effect of ozone-depletion and negative impact on global warming. Although the replacement, hydrochlorofluorocarbons HCFCs (such as HCFC-142b (CF2ClCH3) and HCFC-22 (CHF2Cl), which are used in PS foaming process.) have lower ozone-depletion potential (ODP), they will also be banned by 2010 in the United States. Carbon dioxide (CO_2) is a good substitution for these hazardous blowing agents because it is cheap, nontoxic, nonflammable, and environmentally benign. Yet CO_2 has relatively low solubility and high diffusivity in polystyrene, which makes it difficult to obtain low foam density and small cell size.

The well dispersed nanoparticles in polymer matrix are found to be good heterogeneous nucleation agents for bubble generation [1-4]. Montmorillonite (MMT) is the most widely used one in nanocomposites synthesis. The large surface area combined with its fine dimensions may greatly influence cell nucleation and growth behaviors. But the incompatibility between the MMT surface and polymer matrix largely reduced the capacity for clay to intimately contact with polymer matrix. So MMT surface modification is necessary to prepare well dispersed nanocomposites especially if the polymer matrix has no favorable interaction with the clay surface.

Blending with the polymer which has high CO_2 solubility is another way to increase cell density [5]. However, to obtain uniform morphology from two immiscible polymer blends like PS and PMMA is difficult.

In this study, the CO_2-philic PMMA was grafted on MMT surface by ATRP. PS block was subsequently copolymerized to PMMA to increase the compatibility between the nanocomposites and PS matrix. This copolymerized nanocomposite was melt blended with PS and the mixture was then batch foamed with supercritical CO_2.

Experimental

The initiator of ATRP was synthesized according to the literature [6]. Scheme 1 describes the material used and the synthesis procedure.

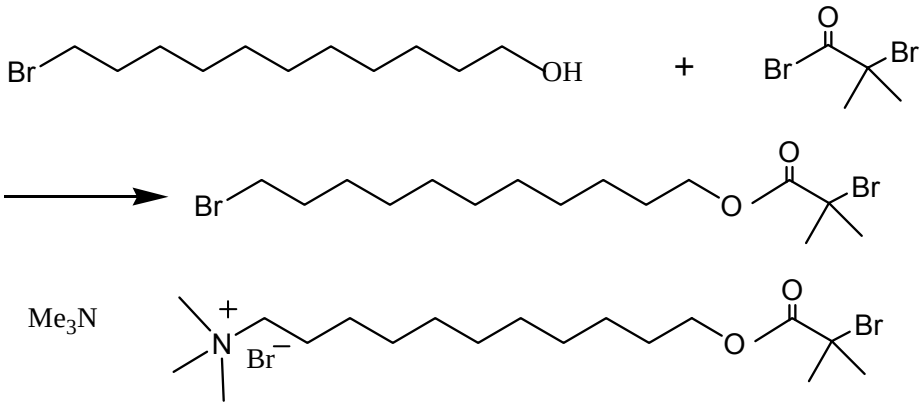

Scheme 1

The synthesized cationic initiator was dissolved in deionized water and drop-wisely added to MMT-water dispersion under vigorous stirring. The exchanged clay was filtered and washed with water and methanol respectively. It was then dried in the vacuum oven at 60^{o}C for 24 hours. The modified clay was ground into fine powders (300 meshes) before use. The amount of immobilized initiator was determined by thermal gravimetric analysis (TGA) as shown in Figure 1.

Graft reactions were carried out in Schlenk flasks equipped with a magnetic stirring bar. Predetermined amount of modified clay, CuBr, 1,1,4,7,10,10-hexamethyltriethylene tetramine (HMTETA) and methyl methacrylate (MMA) were transferred to a Schlenk flask under nitrogen gas. The polymerization was stirred at 90^{o}C for 3h. The Schlenk flask was then subjected to a vacuum to remove unreacted MMA monomer. Styrene monomer was then added to the flask and the polymer was dissolved in styrene monomer. The flask was then heated to 120^{o}C for 6h. The weight percentage of the block copolymer in the nanocomposites can be adjusted by varying the monomer amount. Figure 1 gives an example of 10 wt % nanoclay coated with blockcopolymer measured by TGA. A similar procedure was used to synthesize pure PS-b-PMMA block copolymer except that the initiator was *p*-toluenesulfonyl chloride.

The synthesized nanocomposites or block copolymer was melt blended with PS using DATA mini-twin-screw mixer at 200^{o}C for 5 min. The blends were then compression molded into 1 mm thick, 15 mm diameter disks. For batch foaming, the sample disk was first saturated with supercritical CO_2 at 120^{o}C, 2000 psi for 24h. Then the pressure was quickly released and the sample was put into ice water for 10 min.

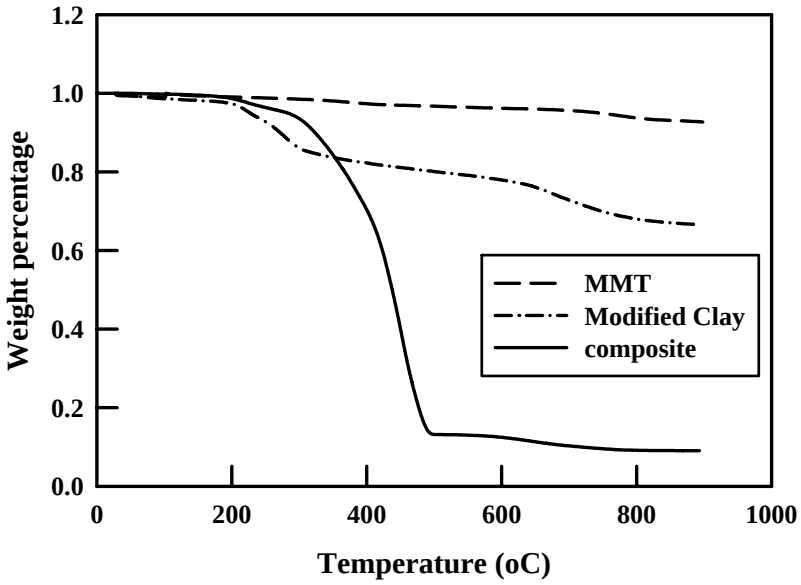

Figure 1. TGA spectrum of MMT, modified clay and PS-*b*-PMMA grafted clay nanocomposite.

Results and Discussion

X-ray diffraction patterns of the MMT, modified clay, and PS-b-PMMA grafted nanocomposite containing 10 wt% of modified clay are shown in Fig. 2. By using the Bragg equation λ=2dsinθ, the d-spacing values of the samples were calculated and shown in Figure 2. The interlayer spacing of MMT increases from d_{001}=1.16 nm to d_{001}=1.88 nm when MMT was modified by the initiator we synthesized. The TGA result from Figure 1 reveals that the initiator content of 25 wt% which corresponds to 0.67 mmol immobilized initiator per g modified clay.

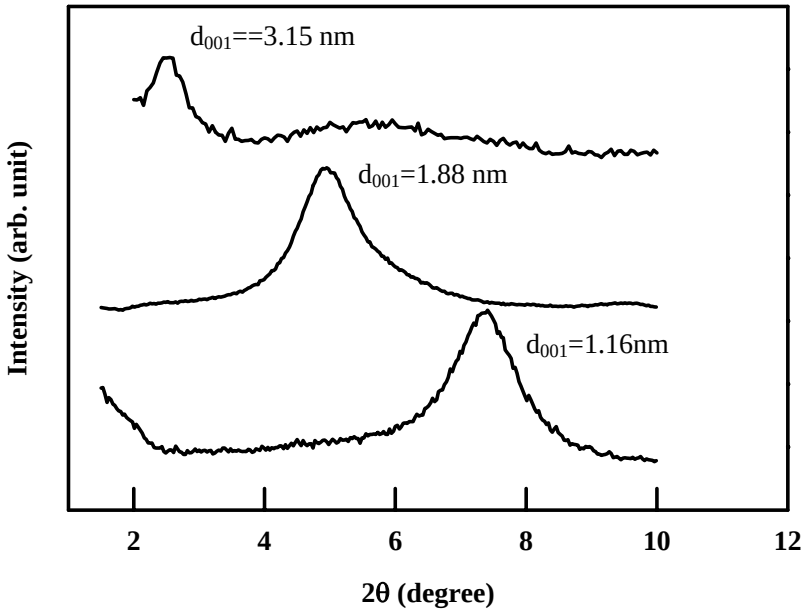

Figure 2. XRD diffraction patterns for (1) MMT; (2) Modified MMT; (3) PS-*b*-PMMA grafted nanocomposites.

After the “living” ATRP of PMMA and PS, the peak around 2θ=5.1 degree become broader and weaker and a new peak at 2θ=2.8 appears, which indicating the further increase of the interlayer distance of the modified clay. TEM image Figure 3a confirmed X-ray’s result. In Figure 3a, it is worth noting that clear phase separation of PS-*b*-PMMA exists in some area. The white area indicates PMMA block and the dark area indicates PS block. According to the sequence of polymerization, all the clay should stay in PMMA phase. Yet we found in Figure 3a that there’s PMMA phase without any clay in it. Although some researchers used very similar polymerization method to make block copolymer nanocomposites,[7-9] no literature has ever published such result. We speculated that during the polymerization, some initiator was detached from the clay surface. The broadened X-ray diffraction peak in Figure 2(3) indicates that the interlayer distance of some of the modified clay becoming smaller after the polymerization. The polymer propagated from detached initiator or the polymer detached from surface becomes free polymer and they may have phase separation depending upon the molecular weight. Apparently, the molecular weight of the polymer we synthesized is large enough to induce the phase separation.

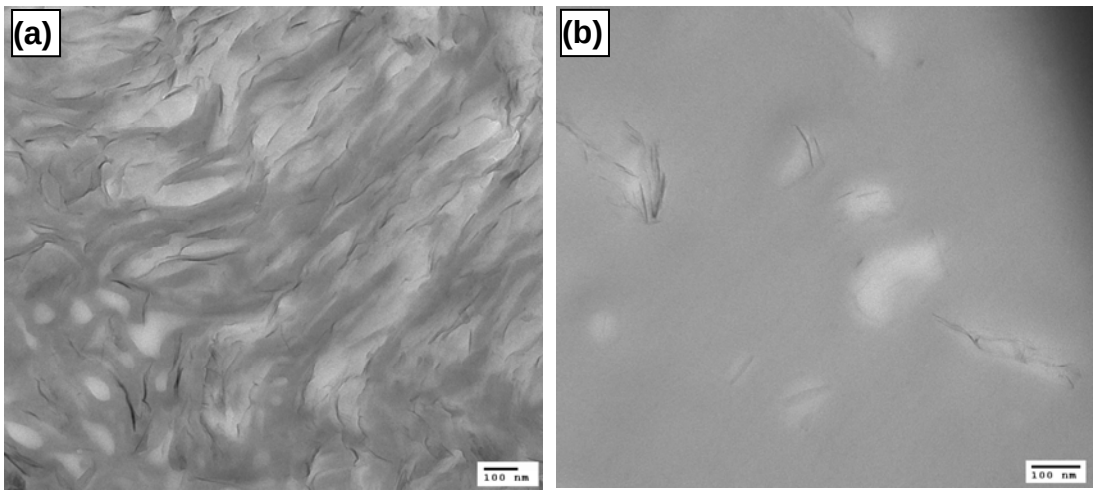

Figure 3. TEM images of (a) PS-b-PMMA grafted nanocomposite and (b) PS/(PS-*b*-PMMA grafted nanocomposite)=9/1 melt blended.

Figure 3b is the TEM image of one melt blended sample of PS and block copolymer nanocomposite described above. It is noticeable that most of the clay stay in the PMMA microdomain and the domain size is around 50-300 nm range. The interface between PS and PMMA is not so clear as the interface between PS and PMMA blends published in the literature.[5] This small microdomain and weak interface separation are attributed to the existence of PS block in nanocomposites. The presence of PS block makes the block copolymer nanocomposite be well dispersed in PS matrix.

Figure 4 shows the complex shear viscosity $|\eta^*|$ versus frequency (ω) for pure PS, PS/PMMA blend, PS/(PS-*b*-PMMA) blend and PS/(PS-*b*-PMMA nanocomposite) blend at 180 ^{o}C. The PS/(PS-*b*-PMMA nanocomposite) blend shows the highest shear viscosity among all the blends. This is reasonable because well dispersed clay has huge surface area. It is interesting that the PS/(PS-*b*-PMMA) blend shows the lowest shear viscosity according to Figure 4. Whether it has some rational behind this or it is just an experimental mistake is still under investigation.

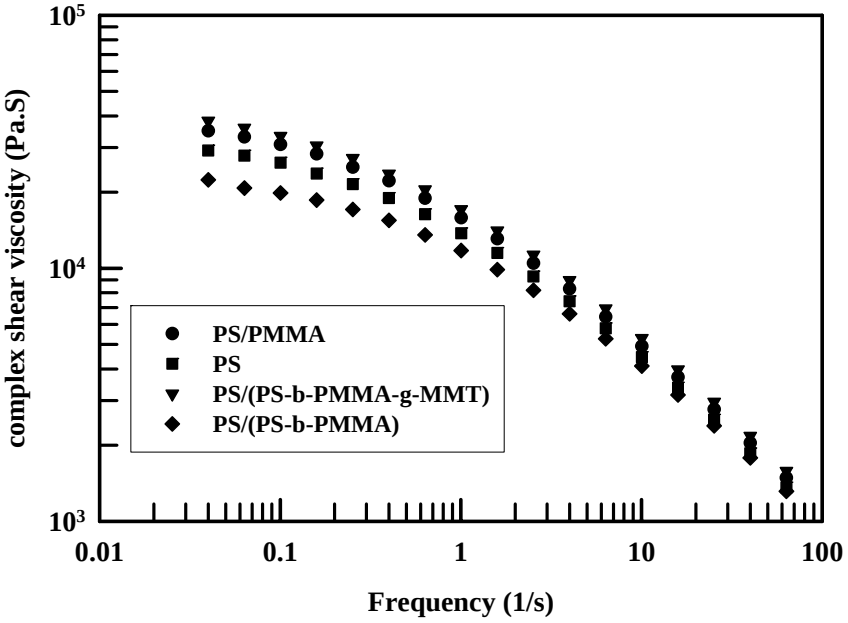

Figure 4. Complex shear viscosity of PS, PS/PMMA blend, PS/(PS-b-PMMA) blend and PS/(PS-*b*-PMMA nanocomposite) blend at 180 ^{o}C.

The pure PS and other three blends described above were all batch foamed in one batch at 120 ^{o}C, 2000 psi. The same batch condition assures that all the materials are foamed at the same saturation condition, same temperature and same pressure release speed. This is important because any condition difference will lead to different foam structure.

Figure 5 shows the foam morphology we obtained from pure PS three blends. In Figure 5 we found that the blend of PS/nanocomposite has the smallest cell size and highest cell density. This observation proves that well dispersed clay which is surrounded by CO_2-philic PMMA is very good heterogeneous nucleation agent. The PS/PMMA blend also has smaller cell size than pure PS. CO_2 has higher solubility in PMMA than in PS which makes the concentration of CO_2 is higher in PMMA under the same saturation condition. High CO_2 concentration means more homogeneous nucleation in PMMA so as to smaller cell size. Han etc. has already showed us that the cell size decreases with the decrease of PMMA domain size in PS/PMMA blends.[5]

One thing abnormal in Figure 5 is that the cell size of PS/(PS-*b*-PMMA) is even larger than pure PS. But this large cell size is consistent with the low viscosity we obtained in Figure 4. It is well known that the higher viscosity, the smaller cell size. Associating the cell size in Figure 5 with the viscosity in Figure 4, we can clearly observe this conclusion. Yet we still need to explain the low viscosity of the PS/(PS-*b*-PMMA) blend.

Conclusion

Well dispersed nanocomposite was prepared by grafting PS-b-PMMA on MMT surface by ATRP. The nanocomposite was then melt blended with PS and then batch

foamed with supercritical CO_2. It was found that the cell size of the foam based on this block copolymer nanocomposite is smaller than pure PS or PS/PMMA blends. The nucleation effect of the nanoparticles surrounded by PMMA is well displayed.

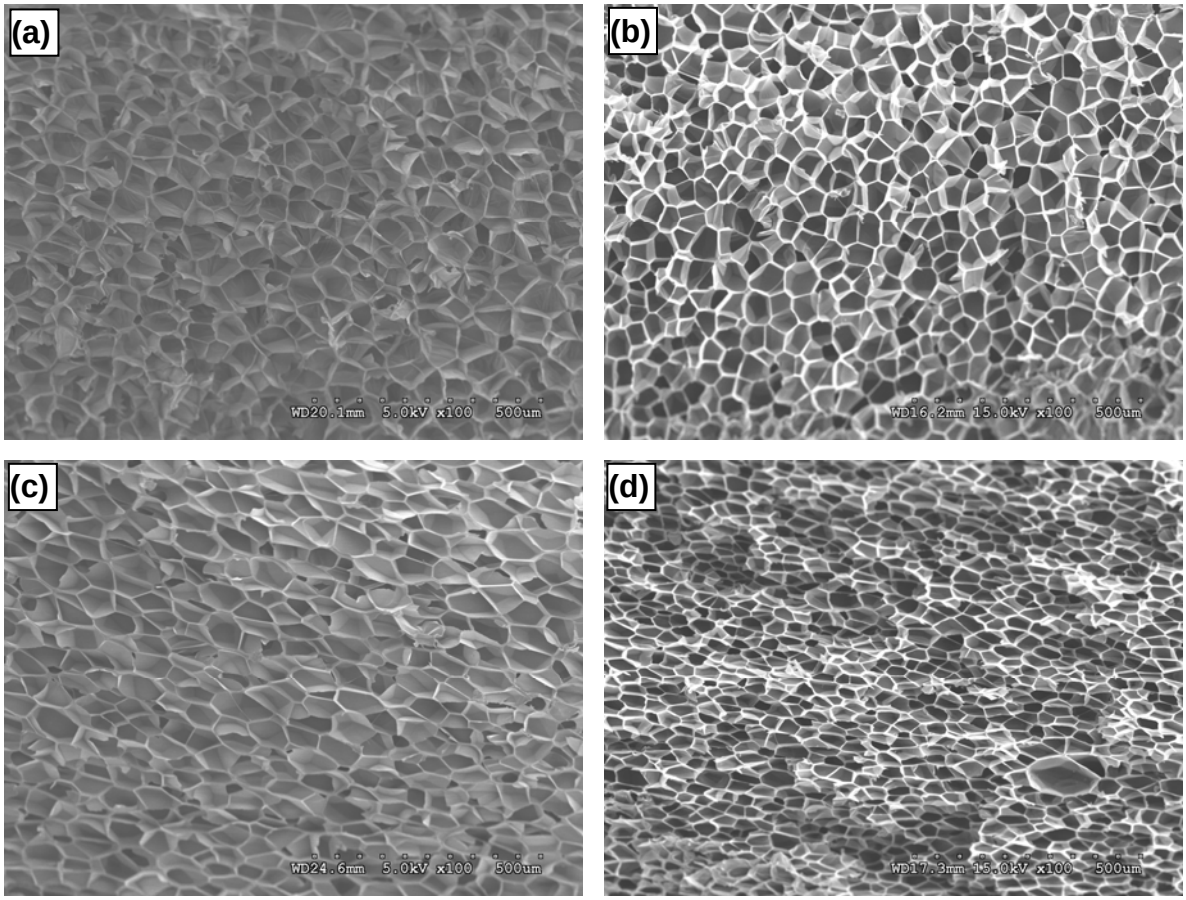

Figure 5. Foam structure at a foaming temperature of 120°C and a saturation pressure of 2000 psi: (a) pure PS (cell size, 54.8 μm; cell density, 1.5×10^7 cells/cc), (b) PS/PMMA(9/1) (cell size 45.9 μm, 17.2 mm; cell density, 1.8×10^7 cells/cc), (c) PS/(PS-*b*-PMMA)(9/1) (cell size 60.4μm, cell density, 1.2×10^7 cell/cc) and (d) PS/(PS-*b*-PMMA nanocomposite) (9/1) (cell size 29.1 μm, cell density, 3.1×10^7 cell/cc)

Literatures

1. P.H. Nam, P. Maiti, M. Okamoto, T. Kotaka, T. Nakayama, M. Takada, M. Ohshima, A. Usuki, N. Hasegawa, and H. Okamoto, *Polym. Eng. Sci.*, 2002, 42,1907.

2. P.H. Nam, M. Okamoto, P. Maiti, T. Kotaka, T. Nakayama, M. Takada, M. Ohshima, A. Usuki, N. Hasegawa, and H. Okamoto, *Nano Lett*., **2001**, 1, 503.

3. C. Zeng, X. Han, L. J. Lee, K. W. Koeling and D. L. Tomasko, *Advanced Materilas*, **2003**, 15, 1743.

4. X. Han, C. Zeng, L.J. Lee, K.W. Koelling, and D.L. Tomasko, *Polym. Eng. Sci*., **2003**, 43, 1261.

5. X. Han, J. Shen, H. Huang, D. L. Tomasko, L. J. Lee, *Polym. Eng. Sci*., **2007**, 47, 103.

6. H. Bo¨ttcher, M. L. Hallensleben, S. Nuß, H. Wurm, J. Bauerb and P. Behrensb, *Journal of materials chemistry*, **2002**, 12, 1351.

7. H. Zhao and D. A. Shipp, *Chem. Mater.* **2003**, 15, 2693.

8. J. Di and D. Y. Sogah, *Macromolecules*, **2006,** 39, 5052.

9. H. Zhao, B. P. Farrell, D. A. Shipp, *Polymer*, **2004**, 45, 4473.